COMPLEX WAVELETS FOR REGISTRATION OF TAGGED MRI SEQUENCES

Estanislao Oubel, Alejandro F. Frangi

Pompeu Fabra University
Department of Technology
Barcelona, Spain
{estanislao.oubel,alejandro.frangi}@upf.edu

Alfred O. Hero

The University of Michigan
Department of EECS
Ann Arbor (MI), USA
hero@umich.edu

ABSTRACT

Tagged Magnetic Resonance Imaging (MRI) is currently the reference MR modality for myocardial motion and strain analysis. MI-based non rigid registration has proven to be an accurate method to retrieve cardiac deformation fields. However, high frequency information in tags is not used. In a previous work this information was included by using feature vectors formed with wavelet coefficients and kNN graphs to estimate αMI. It was shown that cardiac motion estimation was feasible with these features. In this work, features were derived from the complex wavelet transform, which is shift invariant and provides more high frequency subimages than conventional wavelets. The results show that lower errors are obtained with respect to the use of pixel intensity, for both histograms and kNN graphs.

1. INTRODUCTION

Tagged magnetic resonance imaging (MRI) is a well established technique used to obtain regional information on left ventricle (LV) deformation[1], and thus potentially valuable to diagnose cardiovascular diseases. Basically, this technique consists in perturbating the magnetization of the myocardium in a specific spatial pattern at end-diastole. These perturbations appear as dark stripes (tags) when imaged immediately after application of the magnetic field. Since the myocardium retains "memory" of this disturbance, tags undergo the same deformation as the heart does, allowing local strain parameters to be estimated.

Several methods have been proposed to retrieve LV deformation field: optical flow, Harmonic Phase (HARP) MRI, tag detection and tracking, and image registration. The use of MI based non rigid registration to estimate cardiac motion [2] has proven to overcome many drawbacks existent on previous approaches. However, since MI is based on pixel intensity, high frequency information in tags is not accounted for. With the aim of including this information, in a previous work [3] feature vectors formed by wavelet coefficients were used as matching features, and kNN graphs to estimate the αMI between frames of the sequence. In the mentioned work, it was shown that it was feasible to retrieve cardiac motion, but the error obtained with MI was lower.

In this work it was used features vectors formed with the coefficients obtained by applying a complex wavelet transform to the image. This transform is shift invariant and decomposes an image into an approximation and six high frequency subimages. Therefore, it is possible to define for each pixel a vector with additional information on directionality. These features were used along with kNN graphs to improve motion estimation with respect to the classic method based on pixel intensity. The method was tested in four tagged MRI sequences and the results compared against manual measurements.

This paper is organized in six sections. In the next section the Complex Wavelet Transform is introduced. Section 3 explains how to estimate cardiac deformation fields by using image registration. In that section, αMI estimation by using kNN graphs is also presented. Section 4 describes the dataset used for the experiments. Results are presented in Section 5 and discussed in Section 6. Finally, the conclusions can be found in Section 7.

2. COMPLEX WAVELET TRANSFORM

For one dimensional signals, the Discrete Wavelet Transform (DWT) can be regarded as equivalent to filtering a signal with a set of bandpass filters whose impulse responses are scaled versions of a function called mother wavelet. At the coarsest scale, an aditional filter is required to represent the lowest frequencies of the signal. To remove redundancy in the transform, the filter output must be subsampled. The usual way to do this is the cascade filter bank shown in Fig. 1. The bidimensional DWT of an image is obtained applying a 1D DWT to rows and then to columns.

The DWT has two main drawbacks: 1) Lack of shift invariance: this means that the energy of DWT coefficients changes with shifts in the image. For registration purposes it would be desirable for energy to remain the same. 2) Poor directional selectivity: this is a consequence of separable filtering of an image. The Lo-Hi and Hi-Lo filtering provide high

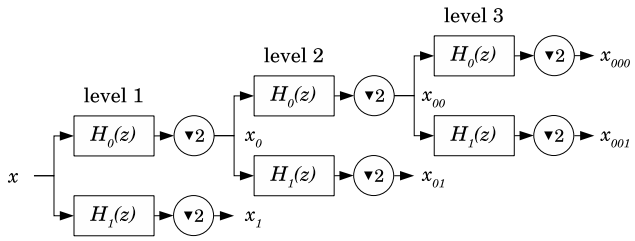

Fig. 1. Filter bank to implement three levels of DWT. H_0: Low pass filter; H_1: High pass filter. An undersampling by 2 is applied to the filter output.

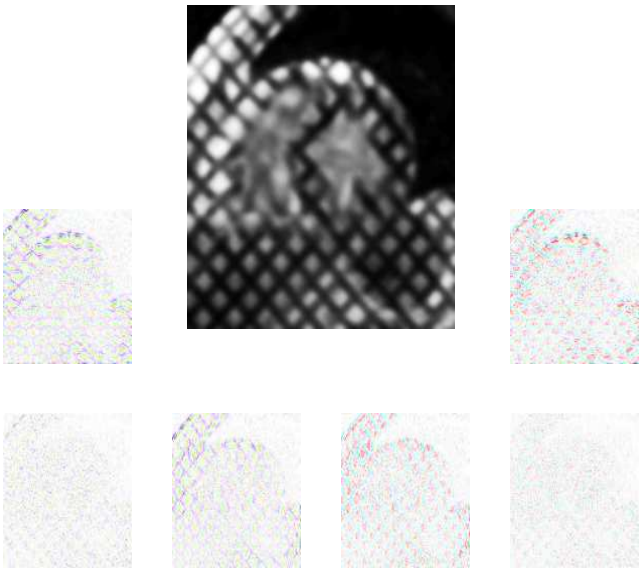

Fig. 2. One-level CWT decomposition of a tagging image. Colors were chosen to represent complex values in the transform.

horizontal and vertical frequencies respectively, and there is no ambiguity in the information. However, the Hi-Hi filtering provides information on diagonal features in both directions (it does not differentiate between an edge at 45^o and 135^o degrees, for example).

To overcome this problems, Kingsbury *et al.* [4] introduced the CWT. This transform can be represented by the same block diagram in Fig. 1, but in this case the filters have complex coefficients and generate complex signals as well. Therefore, a 2:1 redundancy is introduced which results into a 4:1 redundancy for images. Despite being implemented separably, complex filters provide true directional selectivity as they separate all parts of the frequency space. For 2D images the CWT produces six bandpass subimages oriented at $\pm 15^o$, $\pm 45^o$, $\pm 75^o$. A comprehensive explanation and more details on CWT can be found in the paper by Kingsbury *et al.* [5]. Fig. 2 shows the CWT of a tagged MRI image.

3. METHOD

3.1. Motion estimation

To track cardiac motion throughout multiple time frames, Multilevel Free Form Deformations (MFFDs) were used as suggested by Schnabel *et al.* [6], where the transformation $\mathbf{T}(\mathbf{u}, t)$ is represented as the sum of a series of local FFDs:

$$\mathbf{T}(\mathbf{u}, t) = \sum_{p=1}^{t} \mathbf{T}^p_{local}(\mathbf{u}, t)$$

Thus, the motion estimation starts registering the first two frames of the sequence $I(\mathbf{x}, 0)$ and $I(\mathbf{x}, 1)$, and a single FFD is obtained. Then, for the next frame $I(\mathbf{x}, 2)$, a new FFD is added and the frame is registered to $I(\mathbf{x}, 0)$ taking as initial transformation the one obtained for $I(\mathbf{x}, 1)$. This process is repeated for the remaining frames $I(\mathbf{x}, t)$ in the cardiac cycle. Once all the frames are registered to the first one, the MFFD consists of N FFDs that model the myocardium deformation.

The local transformations are obtained by means of the registration algorithm proposed by Rueckert *et al.* [7] for detection of cancerous lesions in contrast enhanced MR breast images. This approach uses MI of pixel intensity to find the transformation that best matches source and target.

The method used in this work proceeds in two steps. First, source and target are registered using CWT aproximation coefficients, and after that, with vectors formed by concatenating detail coefficients taking as input the transformation used in step one. In such a way, the registration process is prevented from being dominated by approximation coefficients, which have higher values than detail coefficients. The last step is where high frequency information in tags is introduced into the registration process. Since feature vectors are in high dimensional spaces, the use of histograms for MI estimation is quite inexact. Therefore, kNN graph estimators were used, which bypass probability function estimation (pdf) estimation.

3.2. αMI estimation using kNN graphs

Given a set $\mathcal{Z} = \{z_1, \ldots, z_n\}$ of n vectors in $\mathbb{R}^d$, the k-Nearest Neighbor Graph (kNN Graph) is formed by the points z_i and the edges with their k nearest points $\mathcal{N}_{k,i}(\mathcal{Z})$. This kind of graph allows the estimation of αMI as explained in the next paragraph.

Let I_s and I_t be two images from which the sets of feature vectors $\mathcal{Z}_s = \{z_{s1}, \ldots, z_{sn}\}$ and $\mathcal{Z}_t = \{z_{t1}, \ldots, z_{tn}\}$ have been extracted. After calculating the corresponding kNN graphs, αMI can be estimated as [8]:

$$\widehat{\alpha MI} = \frac{1}{\alpha - 1} \log \frac{1}{n^\alpha} \sum_{i=1}^{n} \sum_{p=1}^{k} \left(\frac{\|e_{ip}(z_{si}, z_{ti})\|}{\sqrt{\|e_{ip}(z_{si})\| \, \|e_{ip}(z_{ti})\|}} \right)^{2\gamma},$$

where $\|e_{ip}(z_{si}, z_{ti})\|$ is the distance from the point $(z_{si}, z_{ti}) \in \mathbb{R}^{2d}$ to its p-nearest neighbor in $\{z_{sj}, z_{tj}\}_{j\neq i}$, and $\|e_{ip}(z_{si})\|$ ($\|e_{ip}(z_{ti})\|$) is the distance from the point $z_{si} \in \mathbb{R}^d$, ($z_{ti} \in \mathbb{R}^d$) to its p-nearest neighbor in $\{z_{sj}\}_{j\neq i}$($\{z_{tj}\}_{j\neq i}$).

To make a more fair comparison with respect to the results obtained with Shannon MI, ($\alpha\text{MI}|_{\alpha=1}$) was used $\alpha = 0.9$.

3.3. Feature vectors

As commented before in this section, feature vectors at each point in the image were obtained by concatenating wavelet transform coefficients. For DWT, this vectors were formed by grouping corresponding values of LoLo, LoHi, HiLo and HiHi subimages, resulting in points in $\mathbb{R}^4$. When CWT is used, feature vectors are points in $\mathbb{R}^{12}$ (six complex values corresponding to six directional filters).

4. MATERIALS

4.1. Dataset

Four tagged 2D sequences were acquired with a GE Genesis Signa 1.5T MRI scanner. A cine breath-hold sequence with a SPAMM grid tag pattern was used, with imaging being done at end expiration. The in-plane image resolution was 1.56mm×1.56mm. Cardiac cycle was sampled by acquiring a total of 16 frames. However, only images from End of Diastole (ED) to End of Systole (ES) (systolic phase) were used in the experiments due to the interest on evaluating deformation during heart contraction. The length of this cardiac cycle segment is 5 frames.

4.2. Manual measurements

In order to assess the method performance in tracking myocardial motion, tag intersection points were marked manually in each frame by two observers in two independent sessions. For each sequence, 18 points (average) were chosen to be tracked, and thus 90 (18×5) points were marked. Gold standard measurements (GS) were derived for each tag intersection point by taking the average of the measurements made by the observers. Fig. 3 shows the GS point set for each frame in sequence A.

5. RESULTS

The mean error was calculated between the GS and the measurements made by the observers. Table 1 shows the intra and interobserver variabilities of manual landmarking.

The deformation field of the myocardium was calculated with the method explained in Section 3. Fig. 4 shows an example of motion fields obtained and how the landmarks marked by one observer are mapped onto the GS. The resulting transformations were then applied to the GS at ED to map these points to each phase. The mean error between these mapped points and the GS for each phase was calculated. Since this error is different for each phase and in general increases from ED to ES, the sum of this error over all phases was taken as index of method performance. Fig. 5 shows this value for all sequences and methods compared in this work.

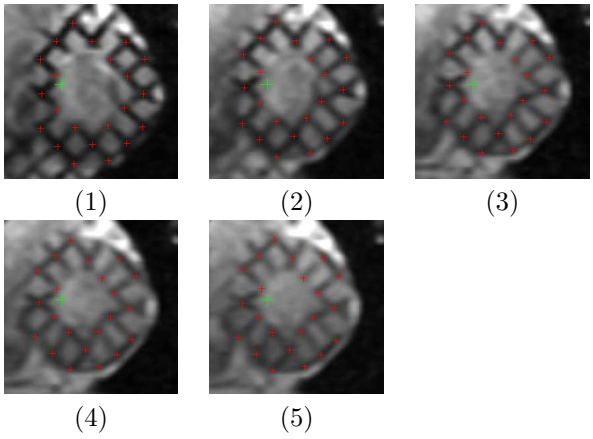

Fig. 3. Gold standard points in each frame from ED to ES for one of the sequences used in this work.

Table 1. Accuracy of manual measurements. Bias and standard deviation of the differences with respect to GS.

	Observer A	*Observer B*	*Observer A and B*
Bias (mm)	0.01	0.06	0.03
SD (mm)	0.35	0.31	0.29

6. DISCUSSION

Fig. 5 shows that for all sequences except B, the use of CWT allowed to obtain lower mean errors than pixel intensity for both histograms and kNN graphs. It is particularly important to note that for most cases CWT and DWT outperform pixel intensity when kNN graphs are used, because the same estimator is used for different features and it allows a more fair comparison on the effect of including high frequency information (the potential effect of using histograms on the per-

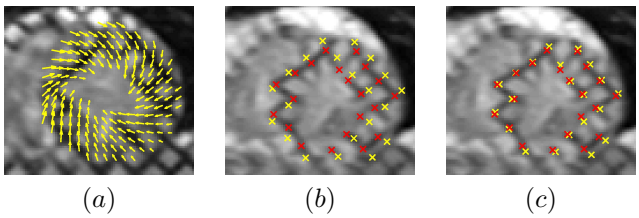

Fig. 4. (a) Motion field from ED to ES. Markers at ES before (b) and after (c) registration

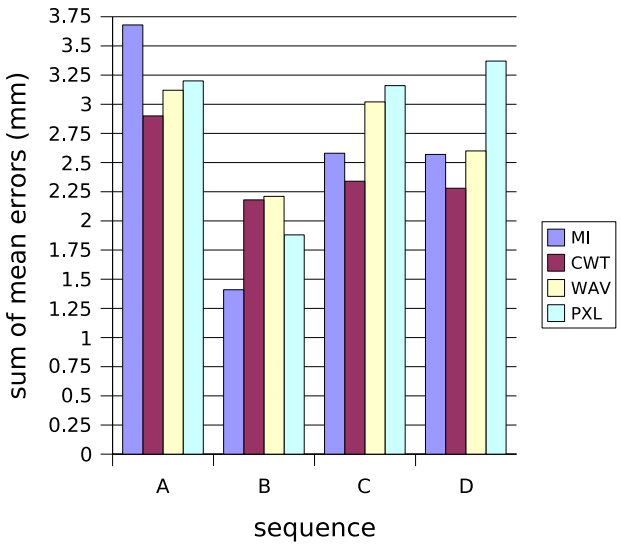

Fig. 5. Sum of mean error over all phases for sequences and metrics used in this work. MI: Standard Mutual Information (pixel intensity and histograms); PXL/WAV/CWT: αMI for Pixel Intensity/Haar Wavelet/Complex Wavelets and kNN graphs.

formance is removed). A possible explanation to the results obtained for sequence B is that this sequence has a very low dynamic range, and therefore tags provide less high frequency information.

The main drawback of the presented method is the speed. The computational burden comes from two sources: calculation of a wavelet transform for each degree of freedom modified during the optimization process, and the use of graphs to estimate αMI. However, whenever features other than pixel intensity are considered the computational cost will be higher, since these features must be calculated someway. With respect to the estimator, some alternatives to kNN graphs are currently being studied and the results will be presented in a future paper.

One possible way of improving the obtained results is the use of CWT phase information, since it depends almost linearly on displacements in the image. Some other ideas are the selection of coefficients based on noise level estimation, and to take advantage of the multiresolution nature of wavelet transform to implement an intrinsically multiresolution method.

7. CONCLUSIONS

High frequency information present in tags has been introduced into a registration based method used for cardiac motion estimation. This has been accomplished by means of CWT, which offers shift invariance, good directional selectivity, and provides a multiresolution image representation intrinsicaly. The use of CWT features allowed to obtain lower errors than Haar wavelet and pixel intensity. However, the computational cost is high, which could limit its practical application (specially in 3D datasets). Currently, the use of CWT phase information, other estimators as alternatives to kNN graphs, and the extension of this method to 3D, are being investigated.

8. REFERENCES

[1] L. Axel and L. Dougherty, "MR imaging of motion with spatial modulation of magnetization," *Radiology*, vol. 171, no. 3, pp. 841–845, 1989.

[2] R. Chandrasheckara, R. H. Mohiaddin, and D. Rueckert, "Analysis of 3D myocardial motion in tagged MR images using non rigid image registration," *IEEE Trans. Med. Imag.*, vol. 23, no. 10, pp. 1245–1250, October 2004.

[3] E. Oubel, C. Tobon-Gomez, A.O. Hero, and A.F. Frangi, "Myocardial motion estimation in tagged MR sequences by using ami-based non rigid registration," in *Medical image computing and computer-assisted intervention - MICCAI 2005*, G. Gerig and J. Duncan, Eds., Palm Springs, CA, USA, October 2005, vol. 3750 of *Lecture Notes in Computer Science*, pp. 271–278, Springer.

[4] N.G. Kingsbury, "The dual-tree complex wavelet transform: a new technique for shift invariance and directional filters," in *Proc. 8th IEEE DSP Workshop*, August 1998.

[5] N.G. Kingsbury, "Image processing with complex wavelets," *Philosophical transactions of the royal society*, vol. 357, pp. 2543–2560, 1999.

[6] J. A. Schnabel, D. Rueckert, M. Quist, J. M. Blackall, A. D. Castellano-Smith, T. Hartkens, G. P. Penney, W. A. Hall, H. Liu, C. L. Truwit, F. A. Gerritsen, D. L. G. Hill, and D. J. Hawkes, "A generic framework for nonrigid registration based on non uniform multi-level free-form deformations," in *Proc. 4th Int. Conf. Medical Image Computing and Computer Assisted Intervention*, W. J. Niessen and M. A. Viergever, Eds., Utrecht, The Netherlands, Oct. 2001, pp. 573–581.

[7] D. Rueckert, L. I. Sonoda, C. Hayes, D. L. G. Hill, M. O. Leach, and D. J. Hawkes, "Nonrigid registration using free-form deformations: application to breast MR images," *IEEE Trans. Med. Imag.*, vol. 18, no. 8, pp. 712–721, Aug. 1999.

[8] H. F. Neemuchwala and A. O. Hero, *Multi-sensor image fusion and its applications*, chapter Entropic graphs for registration, Marcel-Dekker, Inc., 2004.